Well–Defined Amphiphilic Biodegradable Comb–Like Graft Copolymers: Their Unique Architecture-Determined LCST and UCST Thermoresponsivity

4 AUTHORS, INCLUDING:

Gang Wu
University of Electronic Science and Technol…
20 PUBLICATIONS   **211** CITATIONS

Yu-Zhong Wang
Sichuan University
375 PUBLICATIONS   **5,812** CITATIONS

Well-Defined Amphiphilic Biodegradable Comb-Like Graft Copolymers: Their Unique Architecture-Determined LCST and UCST Thermoresponsivity

Gang Wu, Si-Chong Chen, Qi Zhan, and Yu-Zhong Wang*

Center for Degradable and Flame-Retardant Polymeric Materials, College of Chemistry, State Key Laboratory of Polymer Materials Engineering, National Engineering Laboratory of Eco-Friendly Polymeric Materials (Sichuan), Sichuan University, Chengdu 610064, China

ABSTRACT: As an extremely promising characteristic, the transformation between a lower critical solution temperature (LCST) and an upper critical solution temperature (UCST) has rarely been reported until now. In the present paper, a three-step strategy, based on "grafting onto" concept, was implemented to synthesize a novel thermoresponsive amphiphilic biodegradable and biocompatible poly(p-dioxanone)-grafted poly(vinyl alcohol) (PVA-g-PPDO) copolymer with well-define structure. A transformable thermoresponsivity from a LCST to an UCST can be achieved facilely via changing the graft chain length of the resulting PVA-g-PPDO copolymers. The results of transmittance indicate that a wide range of LCST and UCST between 30 and 80 °C can be achieved easily, which is attributed to the controllable structures and hydrophobic/hydrophilic ratio of copolymers by adjusting degree of polymerization (Dp) of PPDO prepolymers and molar feed ratios in the last esterification coupling step. This is the first example having the feature of architecture-determined different-type thermoresponsivities by a facile change of side chain length from an identical comb-like graft copolymer family, and displaying a wide range of controllable LCST and UCST. The influence of solution concentrations on thermoresponsivities has been investigated by UV−vis spectrometer, and the solution properties of copolymers have also been evaluated by dynamic light scattering (DLS). The results show that the self-assembly of copolymers displaying different thermoresponsivities can be observed and regulated by changing the structure and temperature.

Introduction

Thermoresponsive polymers have attracted extensive interests during the past decade because of the potential applications as a "smart materials", especially biomedical applications. Such polymers can be mainly classified into two categories: polymers with a lower critical solution temperature (LCST) above which polymers separate from aqueous solution; and polymers with an upper critical solution temperature (UCST) above which polymers become soluble in water. The polymers having LCST-type phase transition, which are known as water-soluble or hydrophilic polymers, mainly include four types, polymers bearing amide groups, polyethers, polyorgano-phosphazenes and polyphosphoester, respectively.[1−3] In recent a few years, the researches in double-hydrophilic or water-soluble copolymers with these thermoresponsive segments, have attracted great attention because of the temperature-induced self-assembled capability in aqueous[4−9] and the potential applications in many fields such as catalysis,[10−12] nanoreactors manipulation,[13−15] and drug delivery.[16−20] Moreover, thermoresponsive amphiphilic copolymers consisting of hydrophobic segments and LCST-type thermosensitive hydrophilic segments can implement a temperature-induced self-assembly above LCST as well as spontaneously form micelles or vesicles below LCST.[21−24] Owing to their unique self-assembly behaviors and the potential biomedical applications, those kinds of copolymers have attracted more and more attentions,[25−28] especially the copolymers with biodegradability and biocompatibility will be extremely important to considerations for in vivo biomedical applications.[29−32]

Comparing with LCST-type thermoresponsivity, the UCST-type thermoresponsivity is relatively rare. The UCST-type thermoresponsive (co)polymers, such as poly(sulfobetaine),[33] poly(acrylic acid),[34] poly(ethylene oxide)-b-(protonatedP2VP) potassium persulfate complex[35] and poly(2-oxazoline)-based polymers,[36−38] and their micellizations have been reported. For the application in drug controlled release, this type of thermoresponsivity could play an important role, because micelles having UCST can dissolve or dissociate with increasing the temperature, which might lead to the targeted release of encapsulated drugs.[38]

Remarkably, in recent years, a number of dual thermosensitive copolymers consisting of an LCST-type polymer and a zwitterionic polymer presenting a UCST,[39−45] which reveal a core−corona inversion (micelle-unimer-inverse micelle transformation[39,41] or gel−sol−gel transformation[45]) simply depending on temperature, have been reported. For this kind of copolymers, two types of supramolecular interactions, namely hydrogen bonding and electrostatic interactions in aqueous solutions commonly result in the dual thermoresponsivities of both UCST and LCST. Besides, poly(acrylic acid)-based random copolymers displaying the soluble−insoluble−soluble transition which are attributed to intrachain hydrogen-bonding interactions and a moderate hydrophobicity, were reported.[46] Mori et al.[47] synthesized proline-based block copolymers displaying both UCST and LCST and they also demonstrated that thermoresponsivities could be transformed from a system exhibiting LCST and UCST

*To whom correspondence should be addressed: E-mail: yzwang@ scu.edu.cn. Telephone: +86-28-85410259. Fax: +86-28-85410284.

into another one having two different LCSTs by simple methylation reaction.

The transformation between a LCST and a UCST as an extremely promising characteristic has been paid attention. However, only two cases about this feature have been reported until now. For example, Bokias et al.[48] reported that the thermoresponsivities of *N*-isopropylacrylamide/acrylic acid random copolymers could be changed from an UCST to a LCST with increasing the mole fraction of *N*-isopropylacrylamide. Housni et al.[49] reported that a LCST-type solubility change of poly(ethylene oxide)-*block*-poly(*N,N*-dimethylaminoethyl-methacrylate) copolymers on AuNPs was shifted to an UCST-type solubility change by a quaternization of poly(*N,N*-dimethylaminoethyl-methacrylate) block.[49] It is noteworthy that both of them were about linear nonbiodegradable copolymers, and the transformation was achieved by the change of usual thermoresponsive comonomer composition or the structural modification of thermoresponsive polymers, respectively. Moreover, their results do not indicate that the LCST or UCST can be controlled over a wide range, which is quite significant both in theory research and in application.

It has been realized that the architecture of the (co)polymer, including molecular weight and distribution,[50] the type of chain structure such as linear, comb-like, Y-shape, star-like structure, etc.,[51-54] the component of (co)polymer,[41,55] and etc., can play an extremely important role in determining its thermoresponsive phase transition behavior. Hence, for precise evaluation and regulation of their thermoresponsive behaviors, it is essential to synthesize (co)polymers with well-defined molecular structure.

In this work, based on the "grafting onto" concept, a three-step strategy which mainly involved a coupling reaction between macromolecules using carbonyl diimidazole (CDI) as coupling agent, was implemented to synthesize a novel thermoresponsive amphiphilic biodegradable and biocompatible comb-like poly-(*p*-dioxanone)-grafted poly(vinyl alcohol) (PVA-*g*-PPDO) copolymer with well-defined structure. PPDO, as the hydrophobic component of copolymers, is a promising biodegradable and biocompatible aliphatic poly(ether−ester), and has widely been used in biomedical materials.[56,57] PVA, as the hydrophilic component of copolymers, can be biodegraded by many microorganisms (such as *Pseudomonas*, *Alcaligenes*, and *Bacillus* genus),[58] and is safe for organisms.[59,60] Although we have always synthesized PVA-*g*-PPDO amphiphilic comb-like graft copolymers by ring-opening polymerization (ROP) of PDO monomer both in bulk and in solution,[61-63] it is hard to obtain well-defined copolymers because of the poor solubility of PVA in PDO and undesired side reactions such as transesterification and chain transfer reaction between PVA and copolymer.[62] In order to resolve this issue, we introduced the "grafting onto" coupling reaction with CDI as a highly efficient coupling agent.

Extraordinarily, in this study, the unique architecture-determined either LCST-type or UCST-type thermoresponsivity was achieved by adjusting the degree of polymerization (Dp) of the PPDO graft chains. From the viewpoint of molecular structure, this novel thermoresponsive copolymer based on PVA and PPDO is far different from those typical thermo-responsive (co)polymers that have been reported extensively in a number of literatures. To our best knowledge, this report presents the first example having the feature of architecture-determined different-type thermoresponsivities by a facile change of side chain length from an identical comb-like graft copolymer family, and displaying a wide range of controllable LCST and UCST. Considering the unique thermoresponsivity of this copolymer, a new generation of thermoresponsive copolymers could be developed, and the potential applications as biomedical materials would be explored actively.

Experimental Section

Materials. PVA (degree of polymerization 500, degree of hydrolysis 98−99%, M_n = 22 300) was purchased from Alfa Aesar and was used after dried under vacuum at 40 °C until constant weight. PDO (99.9%) with a melt point of 25 °C was provided by the Pilot Plant of the Center for Degradable and Flame-Retardant Polymeric Materials (Chengdu, China), and dried over CaH_2 for 48 h and then distilled under a reduced pressure of 70 Pa just before use. Stannous octoate ($SnOct_2$) (95%) was purchased from Sigma, and was stored in glass ampules under argon after diluted with anhydrous toluene. Carbonyldiimidazole (CDI) (97.16%) was purchased from Asta Tech (Chengdu, China) and purified by recrystallization from anhydrous THF. 4-(Dimethylamino) pyridine (DMAP) (99%) and succinic anhydride (99%) were used as purchased from Nanjin Tianhua Reagent Co. Ltd. (Jiangsu, China) and Bodi Chemical Factory (Tianjin, China), respectively. Other reagents with AR grade were purchased from Bodi Chemical Factory and used for further purification as follows: Isopropanol and triethylamine (TEA) were dried over CaH_2 for 48 h, distilled just before use. THF and toluene were dried by refluxing over Na/benzophenone complex and distilled just before use. Dimethyl sulfoxide (DMSO) was dried over CaH_2 for 72 h, distilled under reduced pressure of 70 Pa just before use. $CHCl_3$ was washed three times by distilled water, dried by refluxing over P_2O_5 and distilled just before use.

Synthesis of PPDO−OH. The PPDO−OH was synthesized through the ring-opening polymerization of PDO initiated by isopropanol. A typical experimental procedure was as follows: Under Ar atmosphere, anhydrous PDO (10.2 g, 0.10 mol) and anhydrous isopropanol (3.0 g, 0.05 mol) were charged into a rigorously dried 50 mL flask which was degassed at 50−55 °C in a vacuum line for 2 h, purging three times with dry nitrogen. After the solution temperature was increased to 80 °C, 0.2 M $SnOct_2$ toluene solution (1 mL, 0.0002 mol) as a catalyst was injected, and the reaction was allowed to proceed for 48 h at 80 °C. The reactors were cooled down rapidly to room temperature. The crude product was dissolved in $CHCl_3$ and then precipitated in anhydrous ethyl ether. After the precipitates were filtered, the products were dried at 40 °C in vacuum until constant weight. The PPDO−OH sample was obtained in 85% yield with Dp = 7 and $M_{n,NMR}$ = 774 (calculated from ^{1}H NMR using eqs 1 and 2, respectively; see Supporting Information). ^{1}H NMR (400 MHz, $CDCl_3$, δ): 5.07 (m, 1H, $(CH_3)_2CHO$), 4.35 (t, 2H, $CH_2CH_2OC(=O)$), 4.18 (s, 2H, $OC(=O)CH_2O$), 4.07 (s, 2H, $CHOC(=O)CH_2O$), 3.80 (t, 2H, $CH_2CH_2OC(=O)$), 3.76 (t, 2H, OCH_2CH_2OH), 3.69 (t, 2H, OCH_2CH_2OH), 1.26 (d, 6H, $(CH_3)_2CHO$). The ^{1}H NMR spectra of the PPDO−OH are shown in Figure S1 (see Supporting Information).

Preparation of PPDO−COOH. The PPDO−COOH was prepared by the acylation of PPDO end-hydroxyl with succinic anhydride using DMAP and TEA as the catalysts. A typical experimental procedure was as follows: First, the dry PPDO−OH (10 g, 0.0129 mol), succinic anhydride (1.42 g, 0.0142 mol) and DMAP (0.96 g, 0.0078 mol) were charged into a rigorously dried 100 mL flask. After the flask was degassed in a vacuum lineand filled with Ar, which was repeated three times, 50 mL of anhydrous $CHCl_3$ was injected using a syringe. When the mixture became homogeneous system, anhydrous TEA (2.0 mL, 0.0142 mol) was charged into flask via a syringe, and the reaction was allowed to proceed for 24 h at room temperature. The crude product was precipitated in anhydrous ethyl ether. Then the precipitate was filtered and dried. This dry product (10 g, 0.0129 mol) was acidized by 0.1 M HCl aqueous solution (129 mL, 0.0129 mol). Finally, the PPDO−COOH with the Dp = 7 and $M_{n,NMR}$ = 874 (calculated from ^{1}H NMR using eqs 1 and 3, respectively; see Supporting Information) was obtained in 90% yield. ^{1}H NMR (400 MHz, $CDCl_3$, δ): 5.07 (m, 1H, $(CH_3)_2CHO$), 4.35 (t, 2H, $CH_2CH_2OC(=O)$), 4.3 (t, 2H, $CH_2CH_2OC(=O)CH_2CH_2COOH$), 4.18 (s, 2H, $OC(=O)CH_2O$),

Scheme 1. Synthetic Route of PVA-*g*-PPDO Copolymers by the "Grafting Onto" Method
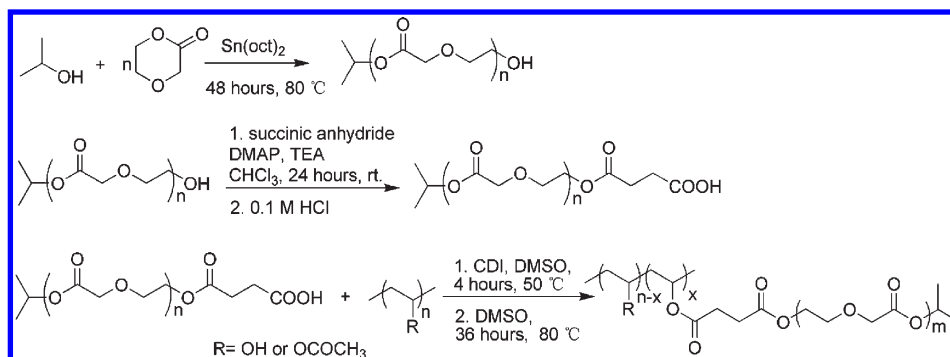
4.07 (s, 2H, CHOC(=O)CH_2O), 3.80 (t, 2H, CH_2CH$_2$OC-(=O)), 2.68 (s, 4H, C(=O)CH_2CH_2COOH), 1.26 (d, 6H, (CH_3)$_2$CHO). ^{1}H NMR (400 MHz, DMSO-d_6, δ): 12.25 (s, 1H, CH$_2$$COOH$), 4.98 (m, 1H, (CH$_3$)$_2$$CHO$), 4.21 (t, 2H, CH$_2$$CH_2$OC(=O)), 4.14 (s, 2H, OC(=O)CH_2O), 4.09 (s, 2H, CHOC(=O)CH_2O), 3.70 (t, 2H, CH_2CH$_2$OC(=O)), 2.57 (s, 4H, C(=O)CH_2CH_2COOH), 1.20 (d, 6H, (CH_3)$_2$CHO). The ^{1}H NMR spectra of the PPDO—COOH are shown in Figure S2 (see Supporting Information).

Synthesis of the PVA-*g*-PPDO Copolymer. The PVA-*g*-PPDO copolymer was synthesized by graft coupling using CDI as coupling agent. A typical experimental procedure was as follows: First, the dry PPDO—COOH (192 mg, 0.2197 mmol) with Dp of 7 and CDI (38 mg, 0.2307 mmol) was charged into a rigorously dried 5 mL flask. After the flask was degassed in a vacuum line and filled with Ar until repeating three times, 1 mL anhydrous DMSO was injected to dissolve the compounds. The flask was heated at 50 °C under Ar atmosphere, and CO$_2$ began to be released. When CO$_2$ was no longer observed after approximately 4 h, the reaction temperature was increased to 80 °C. Meanwhile, 1.5 mL of PVA (100 mg, 0.0045 mmol) anhydrous DMSO solution was injected. The coupling reaction was carried on for 36 h at 80 °C under Ar atmosphere. The reaction mixture was precipitated in methanol, and the precipitate was washed with methanol, CHCl$_3$ and anhydrous ethyl ether, respectively. Finally, the PVA-*g*-PPDO copolymer with the Dg of 8.3% and the Dp of 7 (calculated from ^{1}H NMR using eqs 4 and 5, respectively; see Supporting Information) was obtained in 80% yield (calculated by eq 8; see Supporting Information).

Instrumentation. ^{1}H NMR spectra were measured in CDCl$_3$ or DMSO-d_6 with a Bruker AV II-400 MHz spectrometer. The chemical shifts are given in ppm from tetramethylsilane (TMS) as external standards. The UV—vis spectra were measured by a HITACHI U-1900 spectrophotometer.

The phase transition temperatures (LCST or UCST) of the aqueous soluble or insoluble copolymers with different concentrations were measured by monitoring the transmittance of a 600 nm light beam through a quartz sample cell. The transmittance was recorded on a HITACHI U-1900 spectrophotometer. The control of temperature was conducted by using a PolyScience temperature controller as the heating or cooling instrument. The systems were heated or cooled at a rate of 1 °C/min between 10 and 90 °C, and stabilized for 3 min before the data were recorded.

The variable temperature fluorescence spectroscopy was measured by a HORIBA JOBINYVON Fluormax-4 spectrofluorometer using pyrene (concentration = 6 × 10^{-7} M) as fluorescent probe at a fixed emission wavelength (λ) of 395 nm from 25 to 75 °C. The control of temperature was conducted by using a PolyScience temperature controller as the heating instrument.

DSC measurement was performed with TA Co. Q200DSC (USA) in aluminum pan under nitrogen atmosphere. The samples were preheated up to 150 °C and kept for 5 min to eliminate the thermal history, then cooled to −50 °C. The samples were heated up to 120 °C at the 10 °C/min heating rate. Data were collected during the second heating run.

The average size and size distribution of particles in aqueous solution, after filtered through a Millipore 0.45 μm filter, were measured by dynamic light scattering (DLS) on a Brookhaven model BI-200SM spectrometer and 9000AT correlator using a Innova304 He—Ne laser (1 W, λ = 532 nm) at a fixed scattering angle (θ) of 90° and a correlation measurement time of 2 min with cumulant analysis and CONTIN software. The control of temperature was conducted by using a PolyScience temperature controller as the heating instrument. The systems were heated at a rate of 1 °C/min with a temperature range from 15 to 70 °C, and stabilized for 5 min before the data were recorded.

Results and Discussion

Synthesis of the PVA-*g*-PPDO Copolymer. Generally, the amphiphilic graft copolymer with hydrophilic backbone and hydrophobic aliphatic polyester graft chains could be easily synthesized by ring-opening polymerization of lactones using polyhydroxy polymers as macroinitiator with organometallic catalysts, however, the undesired side reactions (such as transesterification and chain transfer reaction) lead to a poor controllability for the molecular structure.[62,64] To address these issues, a three-step synthesis strategy based on the "grafting onto" concept was utilized to prepare PVA-*g*-PPDO amphiphilic biodegradable graft copolymer as illustrated in Scheme 1. First, PPDO—OH was synthesized through the ring-opening polymerization of PDO initiated by isopropanol. The PPDO—COOH was then synthesized in two processes: the acylation of the end-hydroxyl of PPDO—OH with succinic anhydride in the presence of DMAP and the further treating of this product by 0.1 M HCl aqueous solution, respectively. Finally, the PVA-*g*-PPDO copolymers with various well-defined molecular structures were prepared in DMSO by grafting couple using CDI as coupling agent by esterification between a carboxylic function present on preformed PPDO chain-end and a hydroxyl group naturally present on PVA.
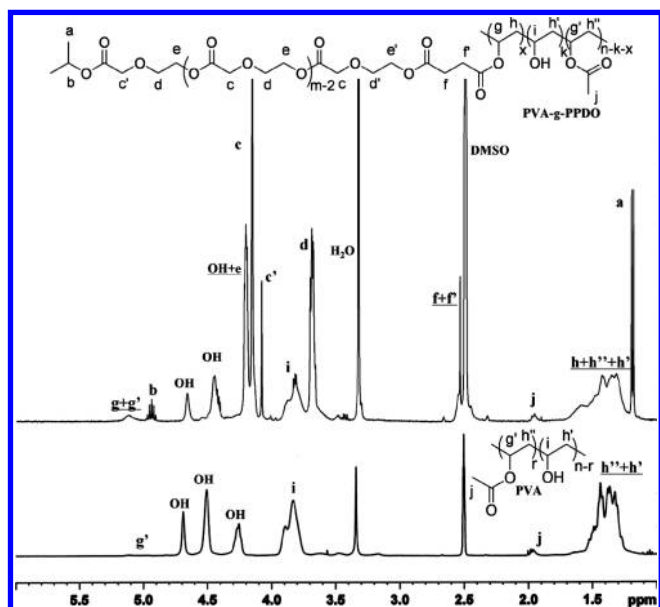
The synthesis of PPDO—OH has been reported in our previous work,[65] and the acylation of the end-hydroxyl of (co)polymers with succinic anhydride has been also achieved successfully.[66] Hence, we performed the first two steps according to the conditions reported previously. The ^{1}H NMR spectra showed that PPDO—OH and PPDO—COOH were obtained as illustrated in Figures S1 and S2 (see Supporting Information). PPDO—OH and PPDO—COOH with various Dp and M_n calculated by NMR have been synthesized (as shown in Table S1).

The coupling reactions between carboxylic group and hydroxyl group in organic synthesis or polymer chemistry using CDI as a high efficient coupling agent (short reaction times, good conversion yields) were reported, especially in the case of polyols and polyesters.[67−69] Despite the fact that dicyclohexylcarbodiimide (DCC) as a coupling reagent and DMAP as a catalyst were used to couple carboxylic group of one macromolecule and hydroxyl group of another one, the

coupling reaction between PVA and PPDO−COOH with DCC/DMAP in DMSO may accompany a facile oxidation of alcohols and cause low grafting yields and conversion yields due to the electrophilic adduct of DCC and low catalytic activity of DMAP in DMSO, respectively.[70−72] Hence, in this work, PVA-*g*-PPDO copolymers were synthesized via a coupling reaction between PVA and PPDO−COOH using CDI as coupling agent in DMSO.

Figure 1 is the ^{1}H NMR spectra of PVA-*g*-PPDO copolymer and neat PVA. Methylene protons of neat PVA and copolymer main chains appeared at 1.25−1.70 ppm and the methine protons that attached to −OH appeared at 3.80−4.00 ppm. The −CH₃ protons of their acetate groups had a characteristic peak at 1.95 ppm. Their hydroxyl protons (−OH) were separated into triads at 4.22/4.47/4.67 ppm. However, for the copolymer, the peaks of methylene groups of PPDO graft chains were visible at 3.70, 4.16, and 4.20 ppm,

and the peaks at 2.55, 1.20, and 4.95 ppm corresponded to the methylene protons of succinate segments, the methyl protons and the methine protons of isopropyl groups connecting to the PPDO chain end, respectively. The proton signals at 5.00−5.30 ppm, corresponding to the methine groups of PVA connected with the ester bond of PPDO chain end, could be used to identify whether the PPDO chains were grafted onto the PVA, because of no obvious signals for pure PVA at 5.0−5.3 ppm.

PPDO−COOH with different Dp, typically 7, 10, 13, and 15, were used to produce a series of amphiphilic graft copolymers with well-defined Dg and Dp, and they were named PVA$_n$-g_x-PPDO$_m$ with *n*VA units, *x* grafted PPDO side chain, and average *m* PDO units per PPDO side chain. For example, the meaning of PVA$_{500}$-$g_{5.6}$-PPDO$_{15}$ is that this copolymer has 500 of VA units, 5.6% of Dg, and 15 of Dp of PPDO side chain. The results are listed in Table 1. For all of the copolymers, the average Dp of PPDO side chains had the same values as those of corresponding PPDO−COOH prepolymers, suggested that there was no side reactions such as the chain extending and degradation, which may lead to change in Dp of PPDO side chain during coupling, and the Dp of copolymers could therefore be controlled by using


Figure 1. ^{1}H NMR spectra of PVA-*g*-PPDO copolymer and PVA in DMSO-*d₆*.
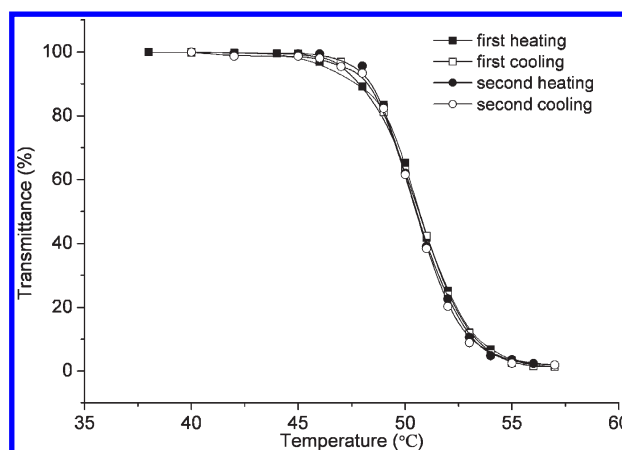
Figure 2. Transmittance versus temperature curves from PVA$_{500}$-$g_{7.6}$-PPDO$_7$ aqueous solution with repeated heating and cooling cycles (concentration = 4.0 mg mL^{-1}).

Table 1. Molecular Characterization of PVA-*g*-PPDO Copolymers [a]

sample[b]	Dp[c]	OH/COOH[d]	Dp[e]	Dg[f] (%)	F_{PPDO}[g](%)	M_n[h] (1×10^4)
PVA$_{500}$-$g_{3.0}$-PPDO$_7$	7	20/1	7	3.0	30.5	3.51
PVA$_{500}$-$g_{5.3}$-PPDO$_7$	7	17/1	7	5.3	42.1	4.50
PVA$_{500}$-$g_{6.2}$-PPDO$_7$	7	14.5/1	7	6.2	45.3	4.88
PVA$_{500}$-$g_{7.2}$-PPDO$_7$	7	10/1	7	7.2	48.4	5.31
PVA$_{500}$-$g_{7.6}$-PPDO$_7$	7	9/1	7	7.6	49.5	5.48
PVA$_{500}$-$g_{8.3}$-PPDO$_7$	7	8/1	7	8.3	51.2	5.78
PVA$_{500}$-$g_{10.0}$-PPDO$_7$	7	6.5/1	7	10.0	54.8	6.51
PVA$_{500}$-$g_{17.4}$-PPDO$_7$	7	5/1	7	17.4	64.2	9.68
PVA$_{500}$-$g_{3.1}$-PPDO$_{10}$	10	20/1	10	3.1	39.2	4.03
PVA$_{500}$-$g_{5.6}$-PPDO$_{10}$	10	17/1	10	5.6	52.1	5.48
PVA$_{500}$-$g_{8.3}$-PPDO$_{10}$	10	8/1	10	8.3	60.0	7.05
PVA$_{500}$-$g_{10.0}$-PPDO$_{10}$	10	6.5/1	10	10.0	63.4	8.04
PVA$_{500}$-$g_{3.0}$-PPDO$_{13}$	13	20/1	13	3.0	44.9	4.43
PVA$_{500}$-$g_{5.6}$-PPDO$_{13}$	13	17/1	13	5.6	58.6	6.34
PVA$_{500}$-$g_{8.1}$-PPDO$_{13}$	13	8/1	13	8.1	65.7	8.17
PVA$_{500}$-$g_{5.6}$-PPDO$_{15}$	15	17/1	15	5.6	62.0	6.91
PVA$_{500}$-$g_{10.0}$-PPDO$_{15}$	15	6.5/1	15	10.0	72.2	10.59

[a] The reactions were carried out under the following conditions: COOH/CDI = 1:1.05, T_1 = 50 °C, t_2 = 36 h, and T_2 = 80 °C (CDI was recrystallized by anhydrous THF). [b] PVA$_n$-g_x-PPDO$_m$: *n* is the degree of polymerization of PVA; *x* is the Dg of copolymers; *m* is the Dp of PPDO side chain. [c] The Dp of PPDO−COOH calculated from ^{1}H NMR using eq 1 (Supporting Information). [d] The OH/COOH is the molar feed ratio of hydroxyl groups of PVA and PPCO−COOH. [e] The average degree of polymerization of PPDO side chain, calculated from ^{1}H NMR using eq 5 (Supporting Information). [f] The degree of graft of copolymer, calculated from ^{1}H NMR using eq 4 (Supporting Information). [g] The PPDO weight fraction of copolymer was calculated by ^{1}H NMR from eq 7 (Supporting Information). [h] The number-average molecular weight (M_n) of copolymer was calculated by ^{1}H NMR from eq 6 (Supporting Information).
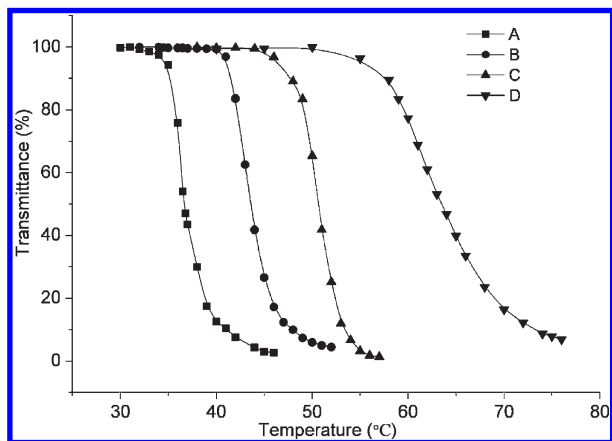
Figure 3. Influences of Dg on the temperature dependence of transmittance changes for 4.0 mg mL^{-1} of aqueous solutions of copolymers: (A) PVA$_{500}$-$g_{10.0}$-PPDO$_7$, (B) PVA$_{500}$-$g_{8.3}$-PPDO$_7$, (C) PVA$_{500}$-$g_{7.6}$-PPDO$_7$, and (D) PVA$_{500}$-$g_{7.2}$-PPDO$_7$.
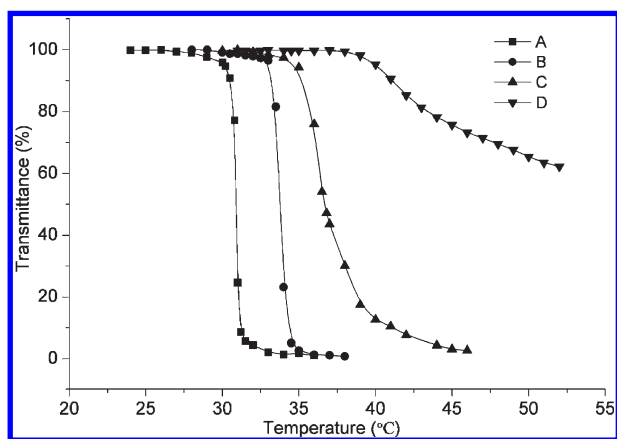

Figure 4. Temperature dependence of the transmittance of PVA$_{500}$-$g_{10.0}$-PPDO$_7$ aqueous solution with different concentrations: (A) 10 mg mL^{-1}, (B) 6 mg mL^{-1}, (C) 4 mg mL^{-1}, and (D) 2 mg mL^{-1}.

prepolymers with different polymerization degrees. In addition, the Dg of PVA-*g*-PPDO copolymers was directly determined by the feed ratio of PVA and PPDO−COOH (OH/COOH) when the Dp was fixed. Since the Dp of PPDO−COOH and the OH/COOH ratio could be easily adjusted, the molecular structure and the hydrophobic/hydrophilic ratio of the copolymers could be controlled effectively, which therefore provided a convenient and efficient method for the control of thermoresponsivity of copolymers.

Architecture-Determined either LCST or UCST Phase Behavior. As above-mentioned, we prepared the PVA-*g*-PPDO amphiphilic copolymers with various well-defined molecular structures by the facile three-step synthesis strategy based on the "grafting onto" concept. Surprisingly, the copolymers with 7 of Dp exhibited a LCST-type thermoresponsivity, while an UCST-type thermoresponsivity was observed in the copolymers with a Dp more than 7. Although the temperature induced phase transition of PVA aqueous solution consisting of 99% and 89% hydrolyzed PVA has been reported,[73] the phase separation appeared after maintained at the desired temperature for 2 days, and it was extremely hard to adjust critical temperatures over a wide range. To our best knowledge, PVA-*g*-PPDO copolymers are the first example for presenting the transformation between LCST-type and UCST-type thermoresponsivity by the change of side chain length of the graft copolymer.
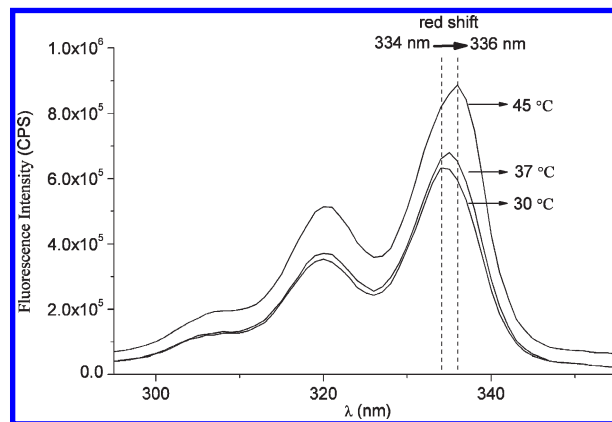

Figure 5. Fluorescence spectra of pyrene in the PVA$_{500}$-$g_{10.0}$-PPDO$_7$ aqueous solution at different temperatures (concentration = 4.0 mg mL^{-1}).
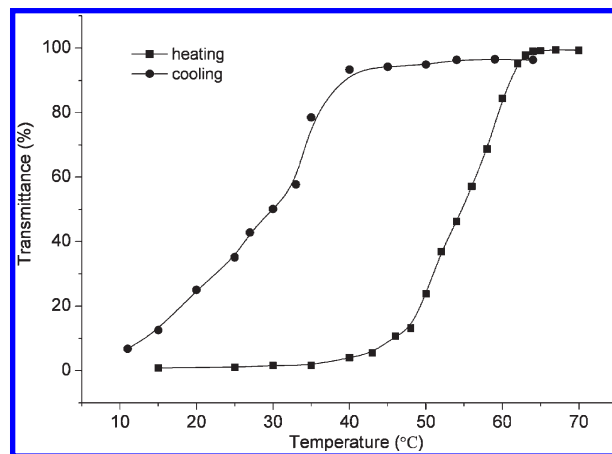
Figure 6. Transmittance versus temperature curves from PVA$_{500}$-$g_{3.0}$-PPDO$_{13}$ aqueous solution with a heating/cooling cycles (concentration = 4.0 mg mL^{-1}).

Although many methods such as the ultrasound resonator technology (URT),[74] were employed to study the thermoresponsivities, the LCST and UCST usually were determined by the measurement of turbidity as a widely used method. The transmittance change of the aqueous soluble or insoluble copolymers with different concentrations in water was monitored on a UV−vis spectrometer at 600 nm between 10 and 90 °C. For those copolymers soluble in water at room temperature, a part of copolymers with 7 of Dp exhibited LCST-type phase transition, and their thermoresponsive behaviors were consistently reversible. Figure 2 shows the transmittance versus temperature curves for PVA$_{500}$-$g_{7.6}$-PPDO$_7$ aqueous solution in repeated heating and cooling cycles. Sharp transition curves can be observed for all temperature cycles, and the curves exhibited a very good coincidence during whole period rather than a hysteresis of change in transmittance between heating and cooling cycle. The results suggest that these copolymers exhibit an extremely sensitive and reversible LCST-type thermoresponsive behavior. In comparison, the phase transition of poly(*N*-isopropylacrylamide) (PNIPAM) aqueous solution for heating and cooling exhibits a strong hysteresis, which was previously reported by Wu et al.[75]

As we know, the LCST of copolymers is influenced strongly by the amphiphilicity of copolymer, and can be controlled by the composition of hydrophobic and hydrophilic units.[76,77] For the PVA-*g*-PPDO copolymer, the LCST
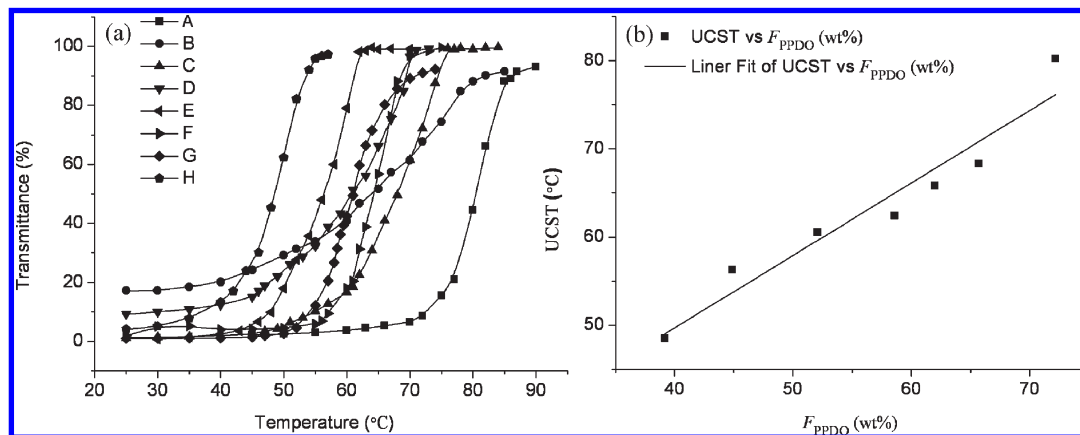
Figure 7. The influences of structural parameters on temperature dependence of transmittance changes for 4.0 mg mL^{-1} aqueous solutions of copolymers (a) and the relationship between the UCST and the weight content of PPDO (F_{PPDO}) of copolymers with a concentration of 4.0 mg mL^{-1}(b): (A) PVA$_{500}$-$g_{10.0}$-PPDO$_{15}$, (B) PVA$_{500}$-$g_{5.6}$-PPDO$_{15}$, (C) PVA$_{500}$-$g_{8.1}$-PPDO$_{13}$, (D) PVA$_{500}$-$g_{5.6}$-PPDO$_{13}$, (E) PVA$_{500}$-$g_{3.0}$-PPDO$_{13}$, (F) PVA$_{500}$-$g_{10.0}$-PPDO$_{10}$, (G) PVA$_{500}$-$g_{5.6}$-PPDO$_{10}$, and (H) PVA$_{500}$-$g_{3.1}$-PPDO$_{10}$.

also was determined by hydrophobic–hydrophilic ratio. No distinctive thermo-responsibility was observed for PVA-*g*-PPDO copolymers with low weight content of PPDO (F_{PPDO}) such as PVA$_{500}$-$g_{3.0}$-PPDO$_7$, PVA$_{500}$-$g_{5.3}$-PPDO$_7$ and PVA$_{500}$-$g_{6.2}$-PPDO$_7$ owning to their relatively high hydrophilicity. The copolymers with high weight content of PPDO (typically PVA$_{500}$-$g_{17.4}$-PPDO$_7$) showed poor water-solubility, and resulted in a visible precipitation during sample preparation. Hence, the copolymers with an appropriate F_{PPDO} endowing the LCST thermoresponsivity were selected, and the influence of their Dg on the LCST was investigated and shown in Figure 3. Comparing the PVA$_{500}$-$g_{7.2}$-PPDO$_7$ with PVA$_{500}$-$g_{10.0}$-PPDO$_7$, both of which have a same Dp of PPDO side chain, the LCST was shifted from 63.0 to 37.5 °C with the increase of Dg. In other words, the LCST decreased with increasing hydrophobicity of the copolymer.

The influence of concentration on the LCST was investigated. As shown in Figure 4, for PVA$_{500}$-$g_{10.0}$-PPDO$_7$ aqueous solution with different concentrations, the LCST decreased with the increase of concentration. Besides, the solutions with higher concentration exhibited sharper transitions, indicating that the sensitivity to temperature changes increased with the concentration of the copolymer. The optical transmittance also increased with the decrease of copolymer concentration.

Considering the mechanism of LCST-type thermoresponsivity for most of the polymers, it is well-known that this thermoresponsive phenomenon generally results from a sensitive balance between advantageous and disadvantageous interactions in water.[78] In regard to PVA-*g*-PPDO copolymers with a low Dg and a certain F_{PPDO}, the hydrogen bonds between the hydroxyl groups of PVA and water or between the ether oxygen of PPDO side-chains and water, as a main driving force, were advantageous to dissolve PVA-*g*-PPDO copolymers into water at room temperature. As temperature increased, these H-bonds were counterbalanced by the increasing hydrophobicity of the apolar backbone of PVA or the ester-bonds of PPDO, which will lead to a spontaneous aggregation of copolymer molecules. Thus, a LCST-type thermoresponsivity was observed for the PVA-*g*-PPDO copolymers in aqueous solution.

In fact, concerning the above-mentioned conjecture, the variable temperature fluorescence spectra of pyrene in the aqueous solution of PVA$_{500}$-$g_{10.0}$-PPDO$_7$ have given evidence as shown in Figure 5. A red shift of the (0, 0) band from 334 to 336 nm was observed with the increase of temperature
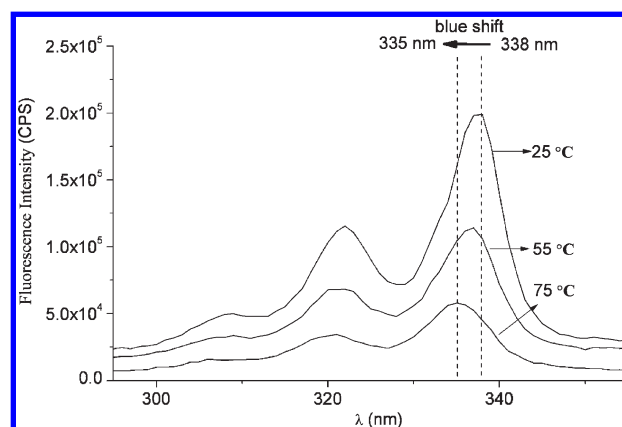

Figure 8. Fluorescence spectra of pyrene in the PVA$_{500}$-$g_{5.6}$-PPDO$_{15}$ aqueous solution at different temperatures (concentration = 4.0 mg mL^{-1}).

from 30 to 45 °C corresponding to the soluble–insoluble change of the copolymer aqueous solution, which suggested that the region around pyrene molecules were changed into more hydrophobic, while there was no any shift of the (0, 0) band for the variable temperature excitation spectra of pyrene in pure water as shown in Figure S4 (Supporting Information).

For the aqueous insoluble systems at room temperature, it is noteworthy that all copolymers with Dp of higher than 7 exhibited a UCST-type phase transition. The reversibility of the phase transition was investigated. Typically, the curves of transmission versus temperature for PVA$_{500}$-$g_{3.0}$-PPDO$_{13}$ aqueous solution at one heating and cooling cycle are shown in Figure 6. Sharp transition curves were observed in both heating and cooling process. However, the curves exhibited a broad hysteresis when cooled, and the value of UCST had a difference of approximate 25 °C for heating and cooling.

When the Dp of copolymers was higher than 7, the UCST-type thermoresponsivity was observed in a wide range of F_{PPDO} from 39.2% to 72.2%. The effect of Dg and Dp of copolymers on the UCST is shown in Figure 7a. Typically, when the Dp of PPDO side chain was fixed at 10, the UCST of PVA-*g*-PPDO copolymers was shifted from 48.5 to 64.5 °C with the increase of Dg from 3.1% to 10.0%, corresponding to the samples, PVA$_{500}$-$g_{3.1}$-PPDO$_{10}$ and PVA$_{500}$-$g_{10.0}$-PPDO$_{10}$. Similarly, when the Dg of copolymers was fixed at 5.6%, the UCST of PVA-*g*-PPDO copolymers increased
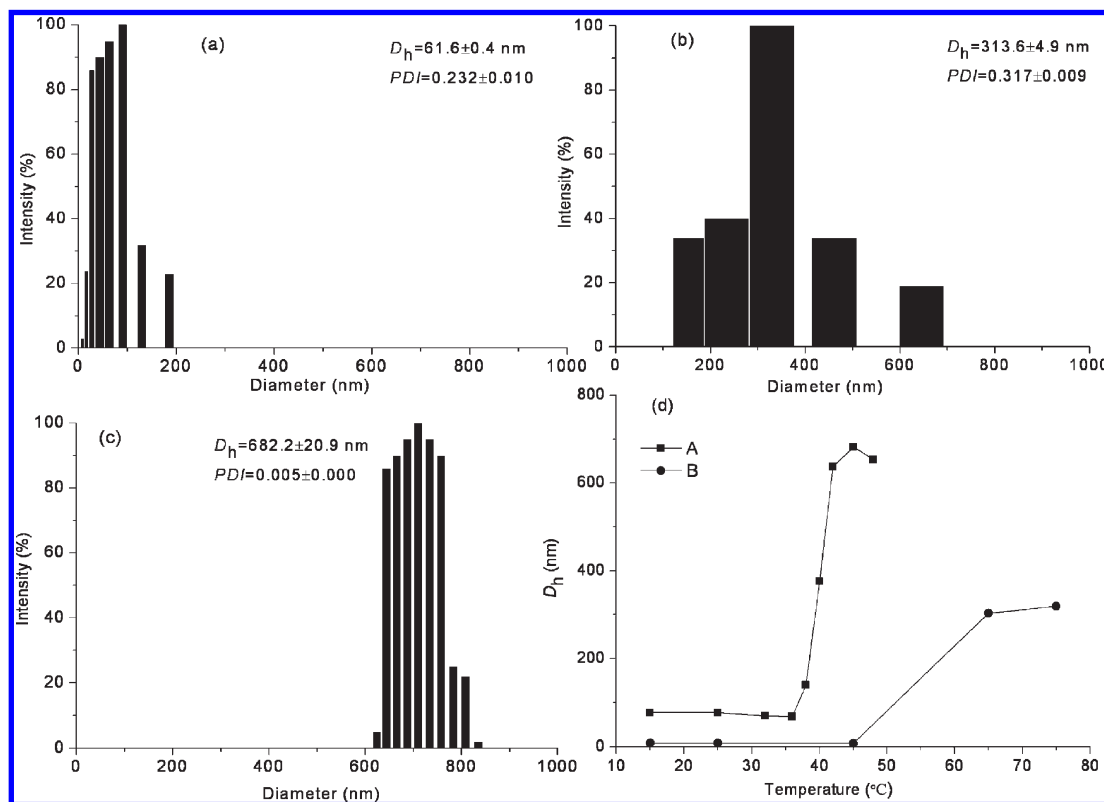
Figure 9. Size and size distribution of aggregates from PVA_{500}-$g_{8.3}$-$PPDO_7$ aqueous solution (concentration = 4.0 mg mL^{-1}) at different temperatures: (a) 32 °C, (b) 40 °C, and (c) 45 °C. (d) Temperature dependence of hydrodynamic diameters (D_h) of aqueous solution (concentration = 4.0 mg mL^{-1}) of PVA_{500}-$g_{8.3}$-$PPDO_7$ (A) and PVA_{500}-$g_{7.2}$-$PPDO_7$ (B).

from 60.5 to 65.8 °C with increasing Dp from 10 to 15, corresponding to the samples PVA_{500}-$g_{5.6}$-$PPDO_{10}$ and PVA_{500}-$g_{5.6}$-$PPDO_{15}$. Furthermore, the relationship between the UCST and F_{PPDO} of copolymers was investigated. As shown in Figure 7b, it can be seen that the UCST almost linearly increased with increasing F_{PPDO} of the copolymer. Accordingly, the UCST can be easy tuned over a wide range by adjusting the F_{PPDO} of the PVA-g-PPDO copolymers.

In general, UCST-type thermoresponsivity corresponding to polyzwitterions is mainly attributed to electrostatic interactions. For our systems, there are two types of supramolecular interactions, namely hydrogen bonding and hydrophobic−hydrophilic interaction, in aqueous solutions. By the investigation of the variable temperature fluorescence spectra of pyrene in the aqueous solution of PVA_{500}-$g_{5.6}$-$PPDO_{15}$ as shown in Figure 8, a blue shift of the (0, 0) band from 338 to 335 nm was observed with the increase of temperature from 25 to 75 °C corresponding to the insoluble−soluble change of PVA_{500}-$g_{5.6}$-$PPDO_{15}$ in water. This means that the region around pyrene molecules became more hydrophilic. For the copolymers with Dp higher than 7, the change of the hydrophilic/hydrophobic balance as one of determining factors contributed to the UCST thermoresponsivity. Because of the dominant hydrophobicity of the ester-bonds of PPDO, the copolymers probably first spontaneously self-aggregated into nano- or micro particles in aqueous solutions under room temperature. With elevating temperature, the copolymers became more hydrophilic, which lead to a thermal induced dissociation and dissolution. Thus, the UCST-type phase transition was observed.

Solution Property of PVA-g-PPDO Copolymers. To further investigate the LCST-type and UCST-type thermoresponsive phenomenon for aqueous solution of amphiphilic grafting copolymer PVA-g-PPDO, thermoresponsive solution properties of the copolymers were characterized using dynamic light scattering (DLS). The hydrodynamic diameters (D_h) of particles at different temperatures were calculated from time-correlation functions by the CONTIN mode, and the polydispersity indices (PDI) of the particles were estimated by use of μ_2/Γ^2 from cumulants analysis.

Parts a−c of Figure 9 show the hydrodynamic diameter and the size distribution of PVA_{500}-$g_{8.3}$-$PPDO_7$ copolymer having a LCST-type thermal behavior below (32 and 40 °C) and above (45 °C) LCST. It can be seen from Figure 9a that copolymers in aqueous solution spontaneously self-aggregated into nanoparticles with 61.4 ± 0.4 nm of D_h and 0.232 ± 0.010 of PDI at 32 °C. Although the D_h and PDI remarkably increased to D_h = 313.6 ± 4.9 nm and PDI = 0.317 ± 0.009 as the solution temperature increased from 32 to 40 °C (Figure 9b), the change of transmittance of PVA_{500}-$g_{8.3}$-$PPDO_7$ aqueous solution can not be observed at the temperatures corresponding to the same range of adjusting temperature as shown Figure 3. Further increase in the solution temperature from 40 to 45 °C resulted in the increase of D_h as shown Figure 9c, and a quite narrow PDI (0.005) was observed for PVA_{500}-$g_{8.3}$-$PPDO_7$ at 45 °C.

Figure 9d shows the dependence of D_h on temperature for PVA_{500}-$g_{8.3}$-$PPDO_7$ and PVA_{500}-$g_{7.2}$-$PPDO_7$. It could be found that the D_h of particles formed in PVA_{500}-$g_{8.3}$-$PPDO_7$ aqueous solution was larger than those of PVA_{500}-$g_{7.2}$-$PPDO_7$ in the whole temperature range. The reason for the increase of D_h with the increase of F_{PPDO} from 48.4 to 51.2 may be that the increase of F_{PPDO} caused the enhancement of hydrophobic interaction, which resulted in formation of more stable particles with large sizes corresponding to a low interface curvature. In addition, correlating the result from DLS with transmittance for PVA_{500}-$g_{8.3}$-$PPDO_7$ aqueous solution, we could find that the system gradually
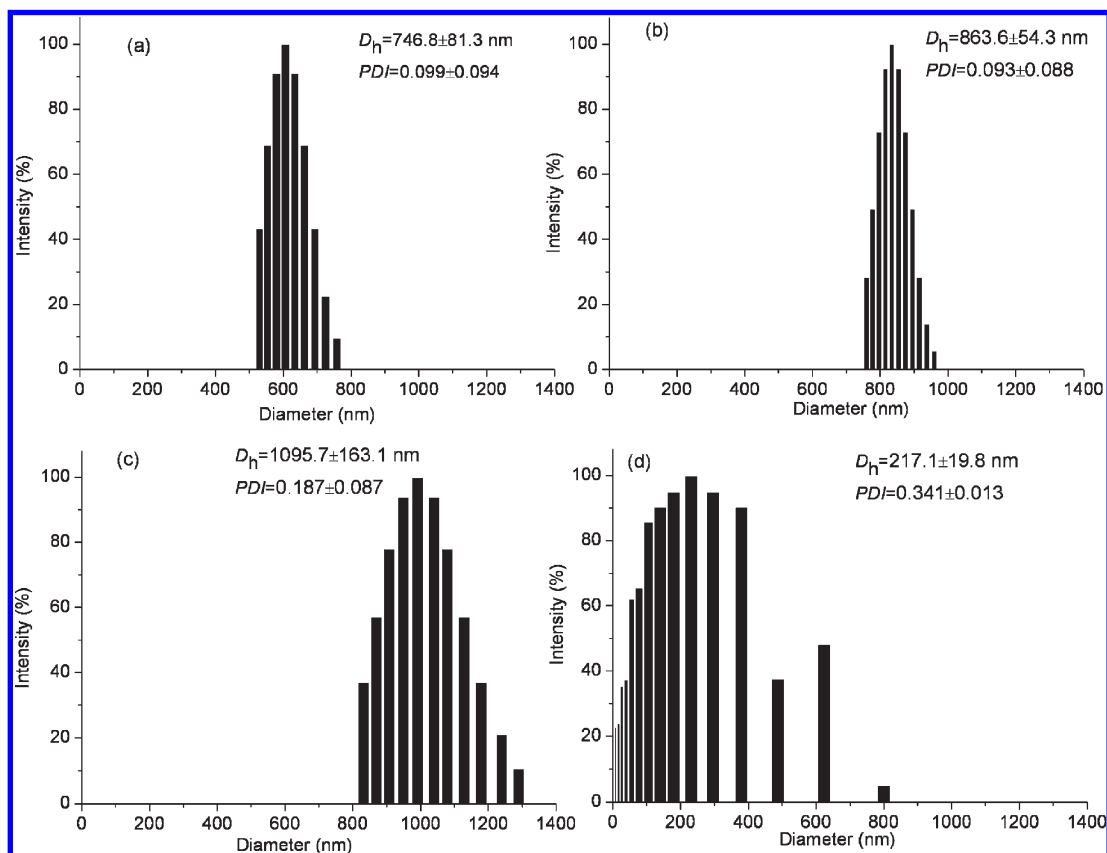
Figure 10. Size and size distribution of aggregates from the aqueous solution (concentration = 4.0 mg mL^{-1}) of copolymers with different structures in different temperatures: (a) PVA$_{500}$-$g_{3.0}$-PPDO$_{13}$ in 25 °C, (b) PVA$_{500}$-$g_{5.6}$-PPDO$_{13}$ in 25 °C, (c) PVA$_{500}$-$g_{8.1}$-PPDO$_{13}$ in 25 °C, and (d) PVA$_{500}$-$g_{8.1}$-PPDO$_{13}$ in 65 °C.
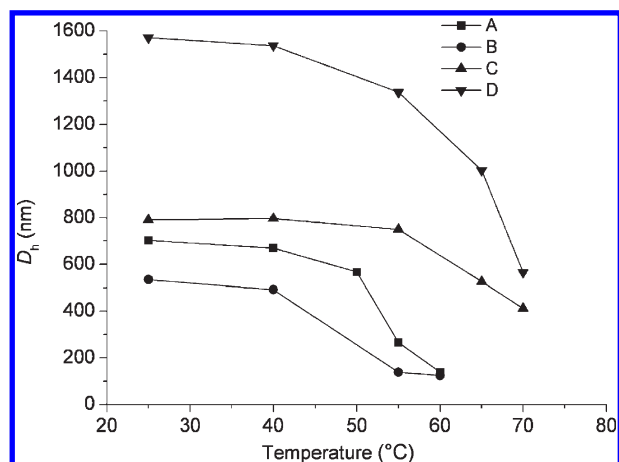

Figure 11. Temperature dependence of D_h of aqueous solution (concentration = 4.0 mg mL^{-1}) of copolymers: (A) PVA$_{500}$-$g_{10.0}$-PPDO$_{10}$, (B) PVA$_{500}$-$g_{5.6}$-PPDO$_{10}$, (C) PVA$_{500}$-$g_{5.6}$-PPDO$_{15}$, and (D) PVA$_{500}$-$g_{10.0}$-PPDO$_{15}$.

became opaque when the solution temperature was above 40 °C, corresponding to the D_h value more than 313.6 ± 4.9 nm. In other words, this result suggests that the emergence of LCST phase transition corresponds to the aggregation of nanoparticles or copolymer molecules with the increase of temperature.

Concerning the solution properties of copolymers displaying UCST-type thermoresponsivity, Figure 10 shows the size and the size distribution of copolymers with a fixed Dp (13) and different Dg's below (25 °C) and above (65 °C) UCST,

Scheme 2. Schematic Representation for the UCST-Type or LCST-Type Thermoresponsive Behaviors of Amphiphilic PVA-g-PPDO Comb-Like Graft Copolymers
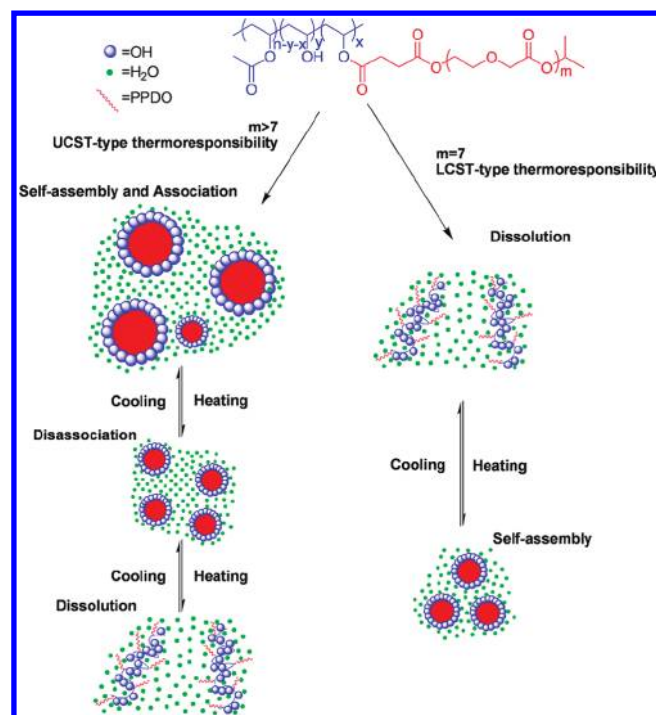
respectively. As shown in parts a and b of Figure 10, at 25 °C, the D_h increased from 746.8 ± 81.3 nm to 863.6 ± 54.3 nm

with increasing Dg from 3.0% to 5.6%, while the PDI was almost unchanged, corresponding to 0.099 ± 0.094 and 0.093 ± 0.088, respectively. To continue increase the Dg from 5.6% to 8.1% resulted in the further increase of D_h from 863.6 ± 54.3 nm to 1095.7 ± 163.1 nm as shown Figure 10b and 10c, and the broader size distribution (0.187 ± 0.087) was observed for PVA_{500}-$g_{8.1}$-$PPDO_{13}$ with 8.1% of Dg. Besides, the sharp decrease in D_h (from 1095.7 ± 163.1 nm to 217.1 ± 19.8 nm) was found for PVA_{500}-$g_{8.1}$-$PPDO_{13}$ with increasing temperature from 25 to 65 °C, corresponding to UCST-type phase transformation. Accordingly, the results indicate that copolymers in aqueous solutions can spontaneously self-assembly into large size aggregates below UCST via hydrophilic−hydrophobic interaction, and the D_h of aggregates can be adjusted by the change of Dg.

Figure 11 shows the D_h versus temperature curves for PVA_{500}-$g_{10.0}$-$PPDO_{10}$, PVA_{500}-$g_{5.6}$-$PPDO_{10}$, PVA_{500}-$g_{10.0}$-$PPDO_{15}$, and PVA_{500}-$g_{5.6}$-$PPDO_{15}$ in aqueous solutions with a same concentration, respectively. For all of four samples, a significant decrease in D_h was observed with the increase of temperature, which may be due to disassociation of aggregates. Comparing the results of PVA_{500}-$g_{10.0}$-$PPDO_{10}$ and PVA_{500}-$g_{5.6}$-$PPDO_{10}$ which have a same Dp and different Dg, the former displayed larger D_h than the latter in the whole range of temperature. On the other hand, when the Dg was fixed at 5.6% or 10.0%, increasing the Dp from 10 to 15 led to the remarkable enlargement of D_h in the whole range of temperature. It is worth noting that the whole curve of D_h versus temperature of PVA_{500}-$g_{10.0}$-$PPDO_{10}$ was below the curve of PVA_{500}-$g_{5.6}$-$PPDO_{15}$ even though the F_{PPDO} of the former was higher than that of the latter. In other words, for the size change of aggregates, the increase of Dp was proved to be more efficient than the increase of Dg, in spite of that copolymers have the nearly same F_{PPDO}. In addition, correlating the results from DLS with transmittance for PVA_{500}-$g_{10.0}$-$PPDO_{15}$ and PVA_{500}-$g_{10.0}$-$PPDO_{10}$ aqueous solutions, the larger D_h corresponded to the lower transmittance, and the decreasing D_h corresponded to the increasing transmittance. Consequently, we suppose that, with the variation of temperature, the macroscopic UCST-type phase transition involves to the change of microscopic particle sizes causing by disassociation and dissolution.

On the basis of the above presented DLS results and the variable temperature fluorescence spectra, the UCST-type or LCST-type thermoresponsive behaviors of PVA-*g*-PPDO copolymers in aqueous solution were schematically shown in Scheme 2. Two processes may be involved mainly in the thermal phase transition of the PVA-*g*-PPDO nano or micro aggregates, namely association-disassociation-dissolution of hydrophobic PPDO segments and formation-breakage of hydrogen bonding of hydrophilic PVA segments. For the copolymers with UCST thermoresponsivity, whose Dp's of PPDO graft chains are higher than 7, the association-disassociation-dissolution of hydrophobic PPDO segments plays an important role in phase transition of the nano or micro aggregates in aqueous medium. Therefore, the copolymer first spontaneously self-aggregated and associated into large size aggregates in aqueous solutions under room temperature via hydrophobic−hydrophilic interaction because of the dominant hydrophobicity from the ester-bonds of PPDO and the crystallization of PPDO chains. With the elevating of temperature, the large size aggregates were gradually disassociated into smaller size aggregates until the dissolution of copolymers, resulting in an increase of optical transmittance. The LCST thermoresponsivity of copolymers with Dp = 7 could be attributed to the breakage of PVA hydrogen bonding. The copolymers with short hydrophobic PPDO chains could

disperse homogeneously in water at room temperature, which was stabilized by the hydrogen bonding between the PVA backbone and the water. With the increase of temperature, the breakage of the hydrogen bonding resulted in an obvious aggregation of the copolymers, and the decrease in optical transmittance was then observed.

Conclusion

The amphiphilic biodegradable and biocompatible PVA-*g*-PPDO comb-like graft copolymers with various well-defined molecular structures were synthesized using a three-step process based on the "grafting onto" concept. In the last step of the process, an optimal coupling condition giving the highest degree of graft (Dg = ~9%) of PVA-*g*-PPDO copolymer and yield (>90%) for the esterifying couple using carbonyl diimidazole (CDI) as a high efficient coupling agent between a carboxylic function of PPDO−COOH and a hydroxyl group of PVA is as follows: COOH:CDI = 1:1.05, T_1 = 50 °C, t_2 = 36 h, and T_2 = 80 °C. Under this condition, the well-defined copolymers with a wide range of Dp (7−15) and Dg (3−17.4%) values were obtained facilely by adjusting the Dp of PPDO−COOH and the molar feed ratio. For this identical comb-like graft copolymer family, the transformation of thermoresponsivity from a quite coincident LCST to a seriously hysteretic UCST can be achieved by changing Dp of PPDO side chain from 7 to more than 7. Furthermore, a wide range of LCST and UCST can be obtained between 30 and 80 °C by the change of concentrations or structural parameters. The temperature-dependent solution properties of the resulting LCST-type or UCST-type copolymers with various structures were influenced strongly by molecular structures. By correlating the result from the variable temperature fluorescence spectra, DSC, and DLS with the transmittance for the copolymers with different-type thermoresponsivities, we suppose that the macroscopic LCST-type or UCST-type phase transition mainly is related to the temperature-induced size change of microscopic particles determined by the hydrophilic/hydrophobic balance and the solid-state property.

Supporting Information Available: Text giving the definition and caluclation of structural parameters, figures showing ^{1}H NMR spectra of the PPDO−OH and PPDO−COOH in CDCl$_3$ or DMSO-d_6, the influence of time on Dg and yield of PVA-*g*-PPDO copolymer, the variable temperature fluorescence spectra of pyrene in pure water, the DSC second heating scan curves of PVA and copolymers, and tables giving the NMR data of PPDO−OH and PPDO−COOH, the results of the coupling reaction conditions, and the DSC data. This material is available free of charge via the Internet at http://pubs.acs.org.

Note Added after ASAP Publication. This article posted ASAP on January 25, 2011. Throughout the paper "thermoresponsibility" has been changed to "thermoresponsivity" and "thermoresponsibilities" to "thermoresponsivities". The correct version posted on February 15, 2011.

References and Notes

(1) Schild, H. G. *Prog. Polym. Sci.* **1992**, *17*, 163–249.

(2) Dimitrov, B.; Trzebicka, B.; Mueller, A. H. E.; Dworak, A.; Tsvetanov, C. B. *Prog. Polym. Sci.* **2007**, *32*, 1275–1343.

(3) Iwasaki, Y.; Wachiralarpphaithoon, C.; Akiyoshi, K. *Macromolecules* **2007**, *40*, 8136–8138.

(4) Chen, G.; Hoffman, A. S. *Nature* **1995**, *373*, 49–52.

(5) Liu, S.; Billingham, N. C.; Armes, S. P. *Angew. Chem., Int. Ed.* **2001**, *40*, 2328–2331.

(6) Schilli, C. M.; Zhang, M.; Rizzardo, E.; Thang, S. H.; Chong, Y. K.; Edwards, K.; Karlsson, G.; Müller, A. H. E. *Macromolecules* **2004**, *37*, 7861–7866.

(7) Li, Y.; Lokitz, B. S.; McCormick, C. L. *Angew. Chem., Int. Ed.* **2006**, *45*, 5792–5795.

(8) Liu, X.; Ni, P.; He, J.; Zhang, M. *Macromolecules* **2010**, *43*, 4771–4781.

(9) Bao, H. Q.; Li, L.; Gan, L. H.; Ping, Y.; Li, J.; Ravi, P. *Macromolecules* **2010**, *43*, 5679–5687.

(10) Bergbreiter, D. E.; Case, B. L.; Liu, Y. S.; Caraway, J. W. *Macromolecules* **1998**, *31*, 6053–6062.

(11) Hamamoto, H.; Suzuki, Y.; Yamada, Y. M. A.; Tabata, H.; Takahashi, H.; Ikegami, S. *Angew. Chem., Int. Ed.* **2005**, *44*, 4536–4538.

(12) Yan, N.; Zhang, J.; Yuan, Y.; Chen, G.-T.; Dyson, P. J.; Li, Z.-C.; Kou, Y. *Chem. Commun.* **2010**, *46*, 1631–1633.

(13) Lu, Y.; Mei, Y.; Drechsler, M.; Ballauff, M. *Angew. Chem., Int. Ed.* **2006**, *45*, 813–816.

(14) Jiang, X.; Xiong, D.; An, Y.; Zheng, P.; Zhang, W.; Shi, L. *J. Polym. Sci., Part A: Polym. Chem.* **2007**, *45*, 2812–2819.

(15) Urbani, C. N.; Monteiro, M. J. *Macromolecules* **2009**, *42*, 3884–3886.

(16) Soppimath, K. S.; Tan, D. C.-W.; Yang, Y.-Y. *Adv. Mater.* **2005**, *17*, 318–323.

(17) Qin, S.; Geng, Y.; Discher, D. E.; Yang, S. *Adv. Mater.* **2006**, *18*, 2905–2909.

(18) Cheng, C.; Wei, H.; Shi, B.-X.; Cheng, H.; Li, C.; Gu, Z.-W.; Cheng, S.-X.; Zhang, X.-Z.; Zhuo, R.-X. *Biomaterials* **2008**, *29*, 497–505.

(19) Bajpai, A. K.; Shukla, S. K.; Bhanu, S.; Kankane, S. *Prog. Polym. Sci.* **2008**, *33*, 1088–1118.

(20) Wei, H.; Cheng, S.-X.; Zhang, X.-Z.; Zhuo, R.-X. *Prog. Polym. Sci.* **2009**, *34*, 893–910.

(21) Hay, D. N. T.; Rickert, P. G.; Seifert, S.; Firestone, M. A. *J. Am. Chem. Soc.* **2004**, *126*, 2290–2291.

(22) Aubrecht, K. B.; Grubbs, R. B. *J. Polym. Sci., Part A: Polym. Chem.* **2005**, *43*, 5156–5167.

(23) Sundararaman, A.; Stephan, T.; Grubbs, R. B. *J. Am. Chem. Soc.* **2008**, *130*, 12264–12265.

(24) Klaikherd, A.; Nagamani, C.; Thayumanavan, S. *J. Am. Chem. Soc.* **2009**, *131*, 4830–4838.

(25) Liu, S. Q.; Tong, Y. W.; Yang, Y. Y. *Biomaterials* **2005**, *26*, 5064–5074.

(26) Chang, C.; Wei, H.; Quan, C. Y.; Li, Y. Y.; Liu, J.; Wang, Z. C.; Cheng, S. X.; Zhang, X. Z.; Zhuo, R. X. *J. Polym. Sci., Part A: Polym. Chem.* **2008**, *46*, 3048–3057.

(27) York, A. W.; Kirkland, S. E.; McCormick, C. L. *Adv. Drug Delivery Rev.* **2008**, *60*, 1018–1036.

(28) Zamana, N. T.; Yang, Y.-Y.; Ying., J. Y. *Nano Today* **2010**, *5*, 9–14.

(29) Jiang, X.; Smith, M. R., III; Baker, G. L. *Macromolecules* **2008**, *41*, 318–324.

(30) Nagahama, K.; Hashizume, M.; Yamamoto, H.; Ouchi, T.; Ohya, Y. *Langmuir* **2009**, *25*, 9734–9740.

(31) Loh, X. J.; Zhang, Z.-X.; Wu, Y. −L.; Lee, T. S.; Li, J. *Macromolecules* **2009**, *42*, 194–202.

(32) Wang, Y.-C.; Li, Y.; Yang, X.-Z.; Yuan, Y.-Y.; Yan, L.-F.; Wang, J. *Macromolecules* **2009**, *42*, 3026–3032.

(33) Huglin, M. B.; Radwan, M. A. *Polym. Int.* **1991**, *26*, 97–04.

(34) Buscall, R.; Corner, T. *Eur. Polym. J.* **1982**, *18*, 967–974.

(35) Jia, X.; Chen, D.; Jiang, M. *Chem. Commun.* **2006**, 1736–1738.

(36) Hoogenboom, R.; Thijs, H. M. L.; Wouters, D.; Hoeppener, S.; Schubert, U. S. *Soft Matter* **2008**, *4*, 103–107.

(37) Lambermont-Thijs, H. M. L.; Hoogenboom, R.; Fustin, C.-A.; Bomal-D'Haese, C.; Gohy, J.-F.; Schubert, U. S. *J. Polym. Sci., Part A: Polym. Chem.* **2009**, *47*, 515–522.

(38) Hoogenboom, R.; Lambermont-Thijs, H. M. L.; Jochems, M. J. H. C.; Hoeppener, S.; Guerlain, C.; Fustin, C.-A.; Gohyac, J.-F.; Schubert, U. S. *Soft Matter* **2009**, *5*, 3590–3592.

(39) Arotçaréna, M.; Heise, B.; Ishaya, S.; Laschewsky, A. *J. Am. Chem. Soc.* **2002**, *124*, 3787–3793.

(40) Virtanen, J.; Arotçaréna, M.; Heise, B.; Ishaya, S.; Laschewsky, A.; Tenhu, H. *Langmuir* **2002**, *18*, 5360–5365.

(41) Weaver, J. V. M.; Armes, S. P.; Bütün, V. *Chem. Commun.* **2002**, 2122–2123.

(42) Maeda, Y.; Mochiduki, H.; Ikeda, I. *Macromol. Rapid Commun.* **2004**, *25*, 1330–1334.

(43) Plamper, F. A.; McKee, J. R.; Laukkanen, A.; Nykänen, A.; Walther, A.; Ruokolainen, J.; Aseyev, V.; Tenhu, H. *Soft Matter* **2009**, *5*, 1812–1821.

(44) Chang, Y.; Chen, W.-Y.; Yandi, W.; Shih, Y.-J.; Chu, W.-L.; Liu, Y.-L.; Chu, C.-W.; Ruaan, R.-C.; Higuchi, A. *Biomacromolecules* **2009**, *10*, 2092–2100.

(45) Hu, J.; Ge, Z.; Zhou, Y.; Zhang, Y.; Liu, S. *Macromolecules* **2010**, *43*, 5184–5187.

(46) Mori, T.; Nakashima, M.; Fukuda, Y.; Minagawa, K.; Tanaka, M.; Maeda, Y. *Langmuir* **2006**, *22*, 4336–4342.

(47) Mori, H.; Kato, I.; Saito, S.; Endo, T. *Macromolecules* **2010**, *43*, 1289–1298.

(48) Bokias, G.; Staikos, G.; Iliopoulos, I. *Polymer* **2000**, *41*, 7399–7405.

(49) Housni, A.; Zhao, Y. *Langmuir* **2010**, *26*, 12933–12939.

(50) Sun, J.; Peng, Y.; Chen, Y.; Liu, Y.; Deng, J.; Lu, L.; Cai, Y. *Macromolecules* **2010**, *43*, 4041–4049.

(51) Chen, G.; Hoffman, A. S. *Macromol. Rapid Commun.* **1995**, *16*, 175–182.

(52) Li, Y.-Y.; Zhang, X.-Z.; Kim, G.-C.; Cheng, H.; Cheng, S.-X.; Zhuo., R.-X. *Small* **2006**, *2*, 917–923.

(53) Wan, L.-S.; Lei, H.; Ding, Y.; Fu, L.; Li, J.; Xu., Z.-K. *J. Polym. Sci., Part A: Polym. Chem.* **2009**, *47*, 92–102.

(54) Park, J.; Moon, M.; Seo, M.; Choi, H.; Kim, S. Y. *Macromolecules* **2010**, *43*, 8304–8313.

(55) Mori, H.; Kato, I.; Endo, T. *Macromolecules* **2009**, *42*, 4985–4992.

(56) Yang, K. K.; Wang, X. L.; Wang, Y. Z. *J. Macromol. Sci.* **2002**, *C42*, 373–398.

(57) Nair, L. S.; Laurencin, C. T. *Prog. Polym. Sci.* **2007**, *32*, 762–798.

(58) Chiellini, E.; Corti, A.; Antone, S. D.; Solaro, R. *Prog. Polym. Sci.* **2003**, *28*, 963–1014.

(59) Lindemann, M. K. In *Encyclopedia of Polymer Science and Engineering*; Mark, H. F., Gaylord, N. G., Eds.; Wiley-Interscience: New York, 1971; Vol. *14*, p 149.

(60) Kaneo, Y.; Hashihama, S.; Kakinoki, A.; Tanaka, T.; Nakano, T.; Ikeda, Y. *Drug Metab. Pharmacokinet.* **2005**, *20*, 435–442.

(61) Chen, S. C.; Wang, X. L.; Wang, Y. Z.; Yang, K. K.; Zhou, Z. X.; Wu, G. *J. Biomed. Mater. Res. Part A* **2007**, *80A*, 453–465.

(62) Chen, S. C.; Wang, X. L.; Yang, K. K.; Wu, G.; Wang, Y. Z. *J. Polym. Sci., Part A: Polym. Chem.* **2006**, *44*, 3083–3091.

(63) Chen, S. C.; Zhou, Z. X.; Wang, Y. Z.; Wang, X. L.; Yang, K. K. *Polymer* **2006**, *47*, 32–36.

(64) Storey, R. F.; Sherman, J. W. *Macromolecules* **2002**, *35*, 1504–1512.

(65) Yang, K.-K.; Wang, X.-L.; Wang, Y.-Z.; Wu, B.; Jin, Y.-D.; Yang, B. *Eur. Polym. J.* **2003**, *39*, 1567–1574.

(66) Lee, S. J.; Han, B. R.; Park, S. Y.; Han, D. K.; Kim, S. C. *J Polym. Sci., Part A: Polym. Chem.* **2006**, *44*, 888–899.

(67) van Dijk-Wolthuis, W. N. E.; Tsang, S. K. Y.; Kettenes-van den Bosch, J. J.; Hennink, W. E. *Polymer* **1997**, *38*, 6235–6242.

(68) de Jong, S. J.; De Smedt, S. C.; Wahls, M. W. C.; Demeester, J.; Kettenes-van den Bosch, J. J.; Hennink, W. E. *Macromolecules* **2000**, *33*, 3680–3686.

(69) Gref, R.; Rodrigues, J.; Couvreur, P. *Macromolecules* **2002**, *35*, 9861–9867.

(70) Pfitzener, K. E.; Moffatt, J. G. *J. Am. Chem. Soc.* **1965**, *87*, 5661–5670.

(71) Fenselau, A. H.; Moffatt, J. G. *J. Am. Chem. Soc.* **1966**, *88*, 1762–1765.

(72) Bamford, C. H.; Middleton, P.; AI-Lamee, K. G. *Polymer* **1986**, *27*, 1981–1985.

(73) Pae, B. J.; Moon, T. J.; Lee, C. H.; Ko, M. B.; Park, M.; Lim, S.; Kim, J.; Choe, C. R. *Korea Polym. J.* **1997**, *5*, 126–130.

(74) Tauer, K.; Gau, D.; Schulze, S.; Hernandez, H. *Polymer* **2008**, *49*, 5452–5457.

(75) Wang, X.; Qiu, X.; Wu, C. *Macromolecules* **1998**, *31*, 2972–2976.

(76) Tachibana, Y.; Kurisawa, M.; Uyama, H.; Kakuchi, T.; Kobayashi, S. *Chem. Commun.* **2003**, 106–107.

(77) Lutz, J.-F.; Akdemir, O.; Hoth, A. *J. Am. Chem. Soc.* **2006**, *128*, 13046–13047.

(78) Lutz, J. -F.; Weichenhan, K.; Akdemir, O.; Hoth, A. *Macromolecules* **2007**, *40*, 2503–2508.